# NOTES AND CORRESPONDENCE

## The Superadiabatic Surface Layer of the Ocean during Convection

A. ANIS AND J. N. MOUM

*College of Oceanography, Oregon State University, Corvallis, Oregon*

18 April 1991 and 27 January 1992

ABSTRACT

Clear identification of the relatively weak superadiabatic potential temperature gradient in the ocean surface layer during convection has been made with the help of intensive vertical profiling measurements at an open-ocean site. In the surface layer the superadiabatic gradient, with a mean value of $-1.8 \times 10^{-4}$ K m$^{-1}$, was a consistent feature of the convective boundary layer persisting throughout each of six consecutive nights. In the well-mixed layer, below the surface layer, the observed potential temperature was nearly constant and turbulent kinetic energy (TKE) dissipation rate approximately balanced the production of TKE by the buoyancy flux through the sea surface. In the surface layer the TKE dissipation rate was systematically larger than the production of TKE predicted by wind stress and mixed-layer similarity scaling.

### 1. Introduction

In comparison to the convective boundary layer (CBL) of the ocean, the vertical structure of the atmosphere during convection is well known (Driedonks and Tennekes 1984; Stull 1988). The structure of the atmospheric CBL consists of four layers, each governed by different physics. At the surface is a thin microlayer of air [O (1 cm)] in which molecular processes dominate: molecular conduction of heat, viscous transfer of momentum, and molecular diffusion of passive tracers are responsible for the transport between the surface and the lowest few millimeters of the atmosphere. The potential temperature ($\theta$) decrease across the microlayer is very large with temperature gradients on the order of $-1 \times 10^4$ K m$^{-1}$. Above the microlayer is an unstable superadiabatic atmospheric surface layer (ASL) [O (10–100 m)] with temperature gradients on the order of $-1 \times (10^{-2}$–$10^{-1})$ K m$^{-1}$ (the terms potential temperature, adiabatic, and superadiabatic are defined in the caption to Fig. 1). Within the ASL large-scale thermal convection is constrained by proximity to the lower boundary and heat transport is by small-scale turbulent eddies; mixing is by forced convection and appears to be explained by Monin–Obukhov similarity scaling (Driedonks and Tennekes 1984; Stull 1988); turbulent fluxes of momentum and heat are constant with height to within 20% throughout the layer (Haugen et al. 1971). Above the ASL is an atmospheric mixed layer [AML; O (1 km)] in which the change of potential temperature with height is small, mixing is dominated by large-scale, convectively driven thermal plumes, and mixing by free convection appears to follow mixed-layer similarity scaling (Stull 1988). Atop the AML is a fourth layer, the entrainment zone, in which intermittent turbulence, overshooting thermals, Kelvin–Helmholtz waves, internal waves, and sometimes clouds may be found.

The oceanic analog to the microlayer is the cool skin (Paulson and Simpson 1981). The cool skin has an average thickness of a few millimeters and temperature gradients of about $-300$ K m$^{-1}$ (Khundzhua et al. 1977). Recent measurements of turbulence during convection have confirmed the existence of well-mixed layers in the ocean (OML for ocean mixed layer; Shay and Gregg 1986; Lombardo and Gregg 1989) and in a freshwater reservoir (Imberger 1985; Brubaker 1987) that appear to obey mixed-layer scaling. However, to date there have been no theoretical or observational studies that provide a consistent framework for an oceanic surface layer (OSL). While there have been hints of anomalously cool water above the mixed layer (Brubaker 1987; Imberger 1985; Shay and Gregg 1986), in each case the temporal and spatial intermittency of these events was not well resolved. If (as suggested by Brubaker 1987) the isolated cool parcels of fluid near the surface in individual profiles represent "thermals" that form at the surface and subsequently sink into the mixed layer, it might be highly improbable to resolve individual events by profiling measurements. This would also be true if these cool parcels are indicative of the coherent structures near the ocean's surface suggested by Soloviev (1990) or Thorpe et al. (1991). To extract the *mean* structure of the surface layer, our approach was to examine a large number of profiles obtained under conditions during which nighttime

*Corresponding author address:* Dr. Jim N. Moum, Oregon State University, College of Oceanography, Oceanography Administration Bldg. 104, Corvallis, OR 97331-5503.

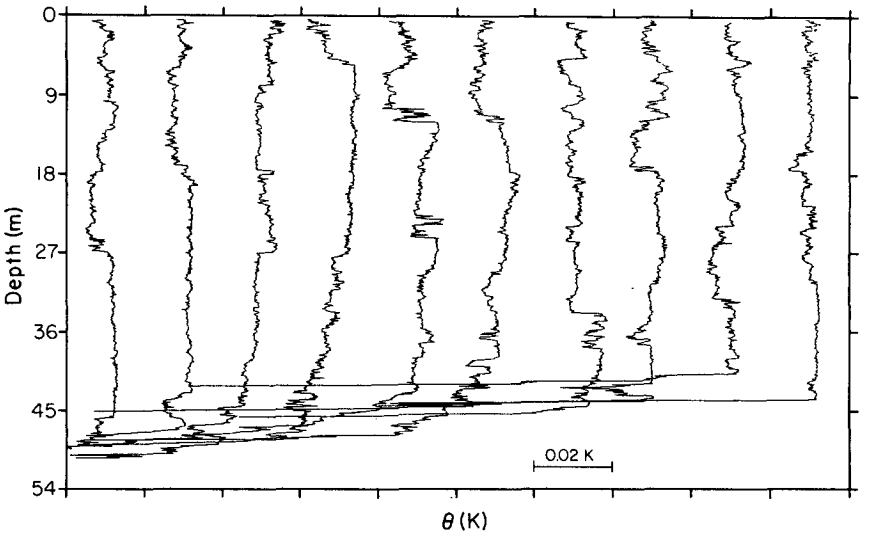


FIG. 1. A typical set of 10 consecutive vertical potential temperature ($\theta$) profiles during nighttime convective conditions. The profiles were taken between local time 0134 and 0239 and the horizontal spacing between profiles is about 900 m. Each profile was referenced to the temperature in the mixed layer by subtracting the average potential temperature in the mixed layer ($-D < z < 2L$). Profiles are offset by 0.02 K. The potential temperature $\theta$ is the temperature the fluid parcel would have if it was expanded or compressed adiabatically (i.e., without thermal contact with the surrounding fluid) from its existing pressure and temperature to a standard reference pressure. This removes the influence of pressure on temperature and is useful when comparing fluid parcels at different depths and when considering vertical motions of fluid parcels. In an adiabatic layer $\theta$ is constant with depth (i.e., a vertical line) and in a superadiabatic layer the vertical derivative of $\theta$, $\partial\theta/\partial z$, is negative.

convection generated a clear mixed layer where TKE dissipation was approximately equal to the surface buoyancy flux. While acknowledging that the physics of the events in the OSL is not well resolved, a consistent mean structure persisting over six separate nights was found. Not entirely unexpectedly, the mean temperature structure of the CBL in the ocean was found to closely resemble that in the atmosphere, at least qualitatively.

Some aspects of the dynamics of the OSL can be deduced from measurements of TKE dissipation rate. It has been suggested (e.g., see Soloviev et al. 1988; Lombardo and Gregg 1989) that, in the OSL, the variation of TKE dissipation rate with depth, $\epsilon(z)$, is proportional to $u_*^3/\kappa z$, the production of TKE by surface winds (where $u_* = \sqrt{\tau/\rho_w}$ is the ocean surface friction velocity, $\tau$ is the surface wind stress, $\rho_w$ is the density of seawater, $\kappa = 0.4$ is von Kármán's constant, and $z$ is positive upward). However, others have found evidence for more intense mixing in this depth range (Kitaigorodskii et al. 1983; Gregg 1987). Our observations indicate $\epsilon(z)$ to be consistently larger than predicted by wind stress and mixed-layer similarity scaling. Although the temperature structure of the OSL mimics that of the ASL, apparently the dynamics do not. Presumably this results from physical processes related to the proximity of a free surface in the OSL that do not apply to the ASL, most studies of which have been made over land.

Experimental details of our investigation are given in section 2, followed by a description of the observations in section 3. In section 4 we discuss the results and show that these are consistent with recent towed temperature measurements by Soloviev (1990) and Thorpe et al. (1991) that have demonstrated some degree of order in a highly variable temperature field.

## 2. Experimental details

As part of the Tropic Heat Experiment in 1987 a large set of hydrographic and turbulence profiles was made from the RV *Wecoma* in the upper Pacific Ocean while steaming south toward the equator. The profiles were made using the Rapid-Sampling Vertical Profiler (RSVP) (Caldwell et al. 1985). The RSVP is a cylindrical free-falling instrument, 120 cm long and 5 cm in diameter, tethered to the ship with a cable serving as data link and retrieval line. This instrument provides near-microscale measurements of temperature and conductivity (from which salinity and density were computed) and microscale velocity fluctuations [from which $\epsilon(z)$ was computed]. The vertical resolution is <1 cm, temperature resolution is 0.5 m K, salinity resolution is $0.6 \times 10^{-3}$ psu, $\sigma_t$ resolution is 0.0004 kg m$^{-3}$, and the noise level of our estimates of $\epsilon(z)$ is less than $1 \times 10^{-9}$ W kg$^{-1}$. Vertical profiles were made to a depth of 200 m at a nominal fall speed of the RSVP of 0.8 m s$^{-1}$ while the ship was moving at about

TABLE 1. Nightly averaged values for the six consecutive nights of the experiment and the mean for all nights (last column). Numbers in parentheses are the 95% confidence intervals of the mean determined using the bootstrap method (Efron and Gong 1983). Wind stress, $\tau$, and surface buoyancy flux, $J_b^0$, were determined from bulk aerodynamic formulas. The depth of the mixed layer, $D$, was determined for each profile and averaged for the night. $L$ is the Monin–Obukhov length scale. It is predicted that convective mixing dominates over the depth range $-D < z \ll L$ when $-D/L \gg 1$. The mean potential temperature gradient ($\partial\theta/\partial z$) of the surface layer for each night was determined for the depth range $2L < z < -0.5$ m. The mean ratio $\epsilon(z)/J_b^0$ was determined over the depth range $-D < z < 2L$. Density values used are $\rho_a = 1.25$ and $\rho_w = 1025$ kg m$^{-3}$ and specific heat values are $C_p^a = 1.0 \times 10^3$ and $C_p^w = 4.0 \times 10^3$ J K$^{-1}$ kg$^{-1}$ for air and seawater, respectively.

| | Night | | | | | | |
|---|---|---|---|---|---|---|---|
| | 1 | 2 | 3 | 4 | 5 | 6 | Mean |
| Number of profiles | 25 | 42 | 78 | 83 | 75 | 63 | |
| $\tau$ (N m$^{-2}$) | 0.08 | 0.10 | 0.08 | 0.07 | 0.11 | 0.11 | 0.09 |
| $J_q^0$ (W m$^{-2}$) | 212 | 211 | 171 | 166 | 205 | 199 | 189 |
| $10^7 J_b^0$ (W kg$^{-1}$) | 1.6 | 1.7 | 1.4 | 1.3 | 1.5 | 1.6 | 1.5 |
| $D$ (m) | 64.4 | 68.5 | 50.6 | 67.5 | 64.3 | 82.2 | 65.1 |
| $L$ (m) | −10.6 | −14.2 | −11.7 | −10.8 | −17.3 | −17.5 | −13.9 |
| $10^4\ \partial\theta/\partial z$ (K m$^{-1}$) | −1.5 | −2.1 | −2.3 | −2.1 | −1.3 | −1.1 | −1.8 |
| | (−2.8, −0.02) | (−2.6, −1.5) | (−2.8, −1.7) | (−2.8, −1.4) | (−1.7, −0.9) | (−1.3, −0.8) | |
| $\epsilon/J_b^0$ | 0.81 | 0.82 | 0.86 | 0.87 | 0.79 | 0.69 | 0.81 |
| | (0.64, 1.00) | (0.77, 0.86) | (0.81, 0.91) | (0.78, 0.95) | (0.74, 0.84) | (0.66, 0.72) | |

2.5 m s$^{-1}$. Time interval between profiles was about 6–7 min. The hydrographic and turbulence measurements were complemented by continuous shipboard measurements of meteorological data. These included wind velocity, air temperature and humidity, solar and longwave radiation, and sea surface temperature and conductivity (C. Paulson and F. Bahr, personal communication). Bulk aerodynamic formulas (Large and Pond 1981) were applied to the surface meteorological data to estimate surface values of wind stress, $\tau$, heat flux, $J_q^0$, and buoyancy flux, $J_b^0$.

## 3. Observations

For the study presented here we have analyzed a series of 366 profiles made over six consecutive nights

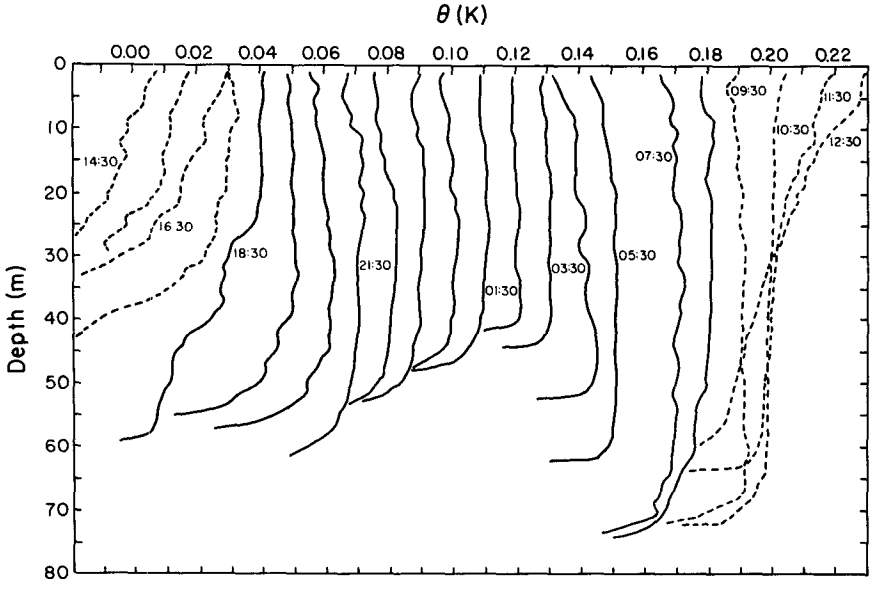


FIG. 2. A sequence of referenced and hourly averaged $\theta$ profiles throughout one diurnal cycle, starting at 1430 local time and ending the following day at 1230. Solid lines are nighttime profiles and broken lines are daytime profiles; profiles are offset by 0.01 K. From this sequence it is observed that the small superadiabatic potential temperature gradient, in the upper part of the profiles, is a persistent feature throughout the night (but away from transition periods). The transition time from $\partial\theta/\partial z > 0$ during daytime, to $\partial\theta/\partial z < 0$ during nighttime (and vice versa) is on the order of 2 hours. The 0630 profile is missing due to instrumentation problems.

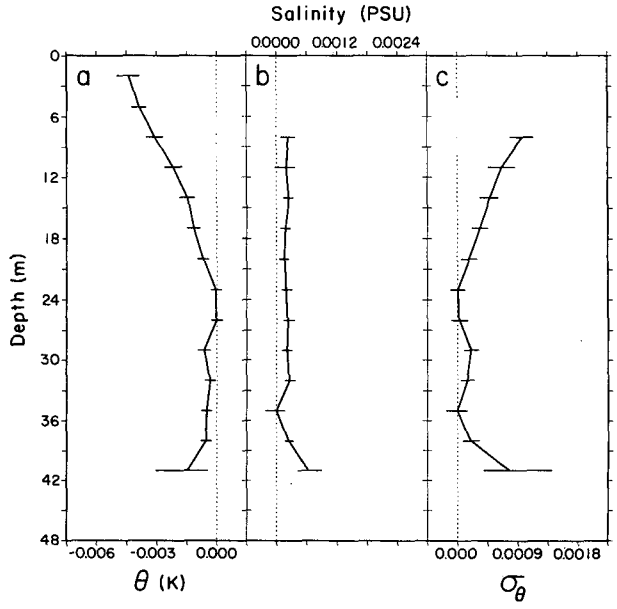


FIG. 3. Referenced and averaged potential temperature, (a) $\theta$, salinity, (b) $S$, and potential density, (c) $\sigma_\theta$ for night 3 (78 profiles); $\theta$, $S$, and $\sigma_\theta$ are plotted relative to their extrema within the mixed layer. Error bars are 95% bootstrap confidence limits. The potential density, $\sigma_\theta$, is calculated from $\theta$ and $S$. The $\theta$ and $S$ scales were chosen to represent equal contributions to $\sigma_\theta$. Salinity values from depths shallower than 6.5 m were omitted due to possible contamination of the conductivity measurements by air bubbles. The weak superadiabatic potential temperature structure of the surface layer has been clearly extracted, by subtracting from each profile the average value of $\theta$ in the mixed layer ($-D < z < 2L$) for each profile, before ensemble averaging into 3-m depth bins. This procedure effectively removed any effects of large-scale horizontal gradients.

during March 1987 along 140°W between 17°N and 7°N. During these nights winds were moderate, varying on average between 7 and 9 m s$^{-1}$, the sea surface losing heat at a nightly rate of 166–212 W m$^{-2}$, and $J_b^0$ was reasonably steady with values of 1.3–1.7 ($\times 10^{-7}$ W kg$^{-1}$). Nightly mean values of mixed-layer depth, $D$, varied between 50.6 and 82.2 m and the Monin–Obukhov length scale, $L = -u_*^3/\kappa J_b^0$ (negative during convection), varied between $-10.6$ and $-17.5$ m (see Table 1).

### a. *Profile-to-profile variability*

A typical set of 10 consecutive vertical profiles of potential temperature made between 0134 and 0239 local time is shown in Fig. 1 (each profile was referenced to the mixed-layer temperature by subtracting the average potential temperature in the mixed layer). The horizontal spatial separation between the profiles is on the order of 900 m. During this section winds were ENE averaging 8–9 m s$^{-1}$ and wind waves and swell had significant wave heights of 0.5 and 2 m, respectively. $J_b^0$ was 1.2–1.3 ($\times 10^{-7}$ W kg$^{-1}$), $L \sim -9$ m, and the depth of the mixed layer was about 45 m. Although some of the profiles show well-mixed sections almost from the sea surface to the base of the mixed layer (e.g., last profile), most of them reveal considerable small-scale variability and complexity. In the fourth, fifth, and sixth profiles from the left, cold water blobs with a vertical extent from the surface to a depth of 5–12 m and with a temperature difference of $-0.01$ to $-0.015$ K, relative to the water below, can be clearly seen. Other profiles (e.g., the second and third from left) show slightly warmer water of about 0.004 K atop cooler water.

### b. *Hourly averages: Diurnal progression*

By averaging the referenced profiles into hourly bins, a clear picture of the temporal development of the oceanic CBL emerges. Figure 2 shows such a sequence throughout one diurnal cycle, starting at 1430 local time and ending the following day at 1230. It is evident that during daytime, when the surface of the ocean is heated by solar radiation, there is a persistent positive potential temperature gradient ($\partial\theta/\partial z$) throughout most of the upper-ocean boundary layer, rendering it statically stable. With the change in sign of surface heat and buoyancy fluxes, during the transition from day to night, $\partial\theta/\partial z$ changes sign from positive to negative in about two hours. $\partial\theta/\partial z$ remains negative throughout the night in the upper 10–25 m (the OSL) until the transition from nighttime to daytime conditions occurs. Between the base of the OSL to the base of the mixed layer the potential temperature is nearly constant, that is, $\partial\theta/\partial z \sim 0$.

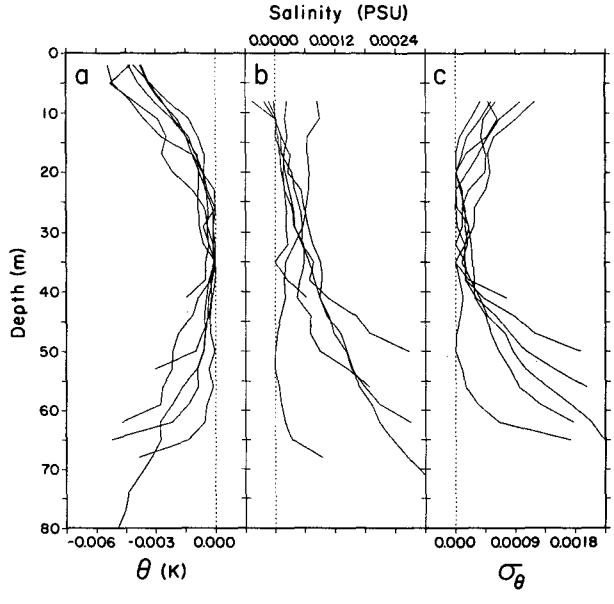


FIG. 4. (a) $\theta$, (b) $S$ and (c) $\sigma_\theta$ for each of the 6 consecutive nights of the experiment. Data were processed and scales were chosen as described in caption to Fig. 3. Extremum values within the mixed layer were subtracted for comparison of profiles.

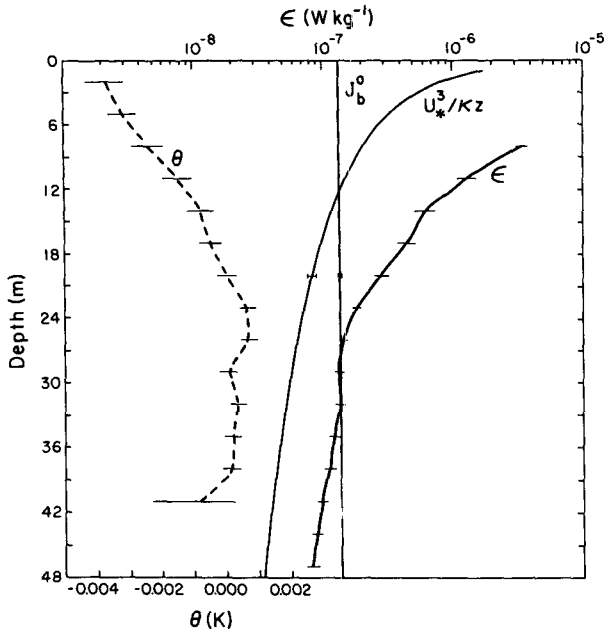


FIG. 5. Referenced and averaged $\theta$ profile and averaged $\epsilon(z)$ profile for night 3. The production terms of TKE by surface winds ($u_*^3/\kappa z$) and by surface buoyancy flux ($J_b^0$) are plotted also. Although $\epsilon(z)$ is reasonably constant within the mixed layer, it is not so in the surface layer. $\epsilon(z)$ increases toward the surface at a greater rate than each or the sum of the production terms ($u_*^3/\kappa z$ and $J_b^0$). $\epsilon(z)$ values from depths shallower than 6.5 m were omitted due to possible contamination by the ship's wake. Error bars are 95% bootstrap confidence limits.

### c. *Mean potential temperature and dissipation profiles during convection*

To examine the mean structure of the oceanic CBL we considered profiles that were made at night, when the ocean surface was losing heat and $J_b^0$ was reasonably steady, starting 2 hours after sunset and ending 2 hours before sunrise. The referenced and averaged potential temperature profile from one particular night indicates the small but significant negative departure from the adiabat between the surface of the ocean and a depth of about 24 m, corresponding to about $2L$ (Fig. 3). Within the superadiabatic layer, salinity was approximately constant within our measurement uncertainty so that potential density ($\sigma_\theta$) changes were determined chiefly by $\theta$, resulting in a statically unstable OSL. Below the OSL, to the base of the OML, $\theta$ more closely followed an adiabat, although variations in $\partial\theta/\partial z$ are apparent. To demonstrate that the superadiabatic OSL was a consistent feature of all six nights in the experiment, we plotted the referenced and averaged profiles together on one plot in Fig. 4. The mean value of $\partial\theta/\partial z$ within the OSL was $-1.8 \times 10^{-4}$ K m$^{-1}$ over the range $2L < z < -0.5$ m (which covered the upper 20–30% of the CBL).

During nighttime, averaged values of $\epsilon(z)/J_b^0$ in the OML indicated a nearly constant value with depth throughout the mixed layer for each of the six nights ($-D < z < 2L$). Nightly means varied between 0.69 ($\pm$0.03) and 0.87 ($\pm$0.09); the mean value over all six nights was 0.81 (Table 1). This value is slightly larger than results from other OML: 0.61 and 0.72 for the Bahamas and ring experiments, respectively (Shay and Gregg 1986), 0.44 to 0.65 during different stages of the development of the diurnal OML (Lombardo and Gregg 1989), and 0.45 from the mixed layer of a freshwater reservoir (Imberger 1985). Although mixed-layer scaling appears to apply within the OML, $\epsilon(z)$ in the OSL is much larger than either the production of TKE by surface winds ($u_*^3/\kappa z$), by surface buoyancy flux ($J_b^0$) or by their sum (Fig. 5), as would be predicted by similarity scaling.

## 4. Discussion and conclusions

The existence of a statically unstable surface layer during convection in the ocean might be simply an

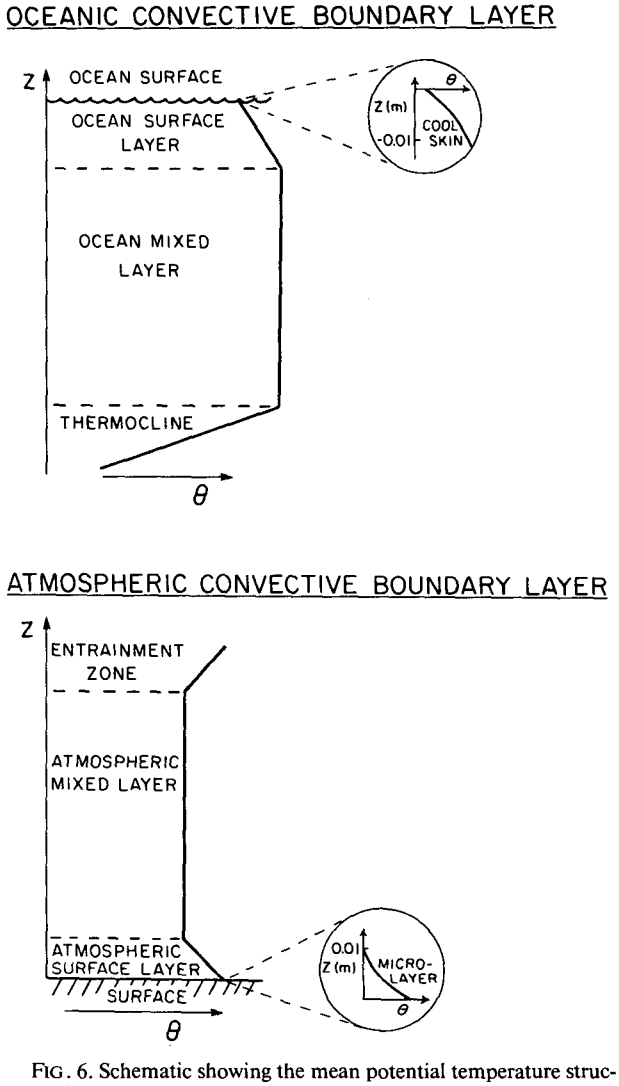


FIG. 6. Schematic showing the mean potential temperature structure of the oceanic and atmospheric CBLs. Table 2 presents a summary of the main characteristics of each layer.

indication of the slow response of the bulk of the mixed layer to changes in surface temperature caused by changing surface fluxes. In cooling the ocean from above, a superadiabatic temperature gradient must appear somewhere in the upper ocean to span the temperature difference across the surface and the mixed layer. In the few millimeters nearest to the surface, molecular conduction (governed by the fluid's molecular diffusivity $D_\theta \approx 1.4 \times 10^{-7}$ m$^2$ s$^{-1}$) is the main heat transfer mechanism, whereas turbulent transport takes over farther away from the surface (i.e., in the OSL). In essence, there *must* be a superadiabatic layer because of the heat loss from the surface of the ocean (mainly due to evaporation) and the inability of the turbulence to mix the entire CBL rapidly enough for complete homogenization.

Towed temperature measurements in the upper ocean have yielded some insight into the horizontal (and vertical) structure of the temperature field near the surface (Soloviev 1990; Thorpe et al. 1991). During both stable (usually daytime) and convective (usually nighttime) conditions, the form of coherent structures in the OSL have been inferred by calculating the skewness, $S$, of the horizontal temperature gradients. Atmospheric and lab measurements in turbulent boundary layers suggest that the sign of the skewness of the temperature gradient measured in the mean-flow direction, $\mathrm{sgn}[S(\partial T/\partial x)]$, is given by $\mathrm{sgn}[\mathbf{x}\cdot(\nabla T \times \omega)]$ (Gibson et al. 1977), where $\mathbf{x}$ is a unit vector in the mean-flow direction, $\nabla T$ is the mean vertical temperature gradient (normal to the boundary), and $\omega$ is the vorticity of the mean flow (in a plane parallel to the boundary). Both studies (Soloviev 1990; Thorpe et al. 1991) found $\mathrm{sgn}(S) > 0$ in the upper few meters of the oceanic CBL. *If* the structure is as shown in their schematic diagrams, with a positive vertical shear of the mean flow, *then* $\mathrm{sgn}[\mathbf{x}\cdot(\nabla T \times \omega)] = \mathrm{sgn}(S) > 0$ *requires* that $\partial T/\partial z < 0$ in the surface layer. Our result of a mean superadiabatic temperature profile (i.e., $\partial\theta/\partial z < 0$) in the OSL during unstable convective conditions is consistent with the prediction of $\partial T/\partial z < 0$ and serves to strengthen the proposed structure of coherent eddies in the OSL presented by these authors.

The high dissipation rates in the OSL suggest an imbalance between the production of turbulence, as predicted by wind stress and mixed-layer scaling, and the rate at which it is dissipated by viscous forces. This apparent imbalance might be explained by additional processes in the OSL due to the proximity to the free surface of the ocean. Near the free surface of the ocean,

TABLE 2. Summary of main characteristics of oceanic and atmospheric convective boundary layers. These are depicted schematically in Fig. 6.

| Layer | Thickness (m) | $\theta_z$ (K m$^{-1}$) | Mixing remarks | References |
|---|---|---|---|---|
| | | Oceanic convective boundary layer | | |
| Cool skin | O (0.01) | $-300$ | molecular diffusion | Khundzhua et al. (1977); Paulson and Simpson (1981). |
| Ocean surface layer | O (10–20) | $-2 \times 10^{-4}$ | $\epsilon/(u_*^3/\kappa z) \gg 1$. Wave breaking, Lagmuir cells, plume formation, shear due to wind stress, and wave drift. | This study. |
| Ocean mixed layer | O (50–100) | $\sim 0$ | $\epsilon/J_b^0 \sim 0.44$–$0.87$. Well mixed by large-scale convective eddies on the order of the mixed layer. Mixed-layer scaling applies. | Shay and Gregg (1986); Lombardo and Gregg (1989); Brubaker (1987); Imberger (1985). |
| Thermocline | O (100–200) | $>0$ | Mean values of $\epsilon < -1 \times 10^{-8}$ W kg$^{-1}$ Intermittent turbulence, internal waves. | |
| | | Atmospheric convective boundary layer | | |
| Entrainment zone | O (100–500) | $>0$ | Intermittent turbulence, overshooting thermals, K–H waves, internal waves. | Stull (1988); Driedonks and Tennekes (1984). |
| Atmospheric mixed layer | O (1–2) $\times 10^3$ | $\sim 0$ | $\epsilon/J_b^0 \sim 0.64$. Well mixed by large convective eddies on the order of the mixed layer. Mixed-layer scaling applies. | Stull (1988); Driedonks and Tennekes (1984); Caughey and Palmer (1979). |
| Atmospheric surface layer | O (10–100) | $-1 \times (10^{-2} - 10^{-1})$ | $\epsilon/(u_*^3/\kappa z) \sim 1 - 2$. Small-scale turbulent eddies created by forced convection. Monin–Obukhov similarity applies. | Stull (1988); Driedonks and Tennekes (1984); Wyngaard and Cote (1971). |
| Microlayer | O (0.01) | $-1 \times 10^4$ | molecular diffusion | Stull (1988). |

wave-induced mean drift may increase effective values of $u_*$ (Churchill and Csanady 1983), Langmuir cells may introduce episodic mixing events (Thorpe 1985; Weller and Price 1988), and surface waves may contribute in a number of ways to intensify turbulence near the surface (Kitaigorodskii et al. 1983; Huang 1986). One or a combination of the aforementioned mechanisms might contribute to additional production of turbulence resulting in the high dissipation rates we observed in the OSL. It is also possible that turbulence and pressure transport terms in the TKE equation may have greater influence than we have previously considered. Thus, the physics governing the mixing is likely to be very complex due to the proximity of a free surface, as is suggested by the vertical structure of $\epsilon(z)$ in the OSL. However, more observations are required to explain the behavior of turbulence in the OSL and its proper scaling under different forcing conditions.

Combining the results of this study with previous results, there appears to be a consistent vertical structure of the oceanic CBL that includes four regimes. Proceeding toward the surface these are the

(i) Stable layer (thermocline) in which $\partial\theta/\partial z > 0$.
(ii) Mixed layer in which $\partial\theta/\partial z \sim 0$ and $\epsilon(z)/J_b^0 \sim$ constant.
(iii) Superadiabatic surface layer in which $\partial\theta/\partial z < 0$ and $\epsilon(z)$ increases toward the free surface more rapidly than accounted for by the production rates of TKE by surface winds and buoyancy flux at the sea surface.
(iv) Cool skin, at the top centimeter or so of CBL, which could not be resolved by our measurements.

The mean value of the potential temperature gradient for all six nights in the superadiabatic layer was $\partial\theta/\partial z \sim -2 \times 10^{-4}$ K m$^{-1}$. Although individual vertical profiles of potential temperature are highly variable within the OSL during convection (Fig. 1), the results of Soloviev (1990) and Thorpe et al. (1991) suggest that the structure has a degree of organization that provides hope in understanding the physics. Our results indicate that the *mean* structure resembles that of the ASL during convection (Fig. 6 and Table 2) and complement observations of time–space variability within the OSL.

*Acknowledgments.* We are grateful to the Captain and crew of the R/V *Wecoma* for their support during the experiment and to Dave Hebert, Murray Levine, and Laurie Padman for their helpful comments. This work was supported by National Science Foundation Grants OCE-8608256 and OCE-8716719.

## REFERENCES

Brubaker, J. M., 1987: Similarity structure in the convective boundary layer of a lake. *Nature,* **330,** 742–745.

Caldwell, D. R., T. M. Dillon, and J. N. Moum, 1985: The rapid sampling vertical profiler: An evaluation. *J. Atmos. Oceanic Technol.,* **2,** 615–625.

Caughey, S. J., and S. G. Palmer, 1979: Some aspects of turbulence structure through the depth of the convective boundary layer. *Quart. J. Roy. Meteor. Soc.,* **105,** 811–827.

Churchill, J. H., and G. T. Csanady, 1983: Near surface measurements of quasi-Lagrangian velocities in open water. *J. Phys. Oceanogr.,* **13,** 1669–1680.

Driedonks, A. G. M., and H. Tennekes, 1984: Entrainment effects in the well-mixed atmospheric boundary layer. *Bound.-Layer Meteor.,* **30,** 75–105.

Efron, B., and G. Gong, 1983: A leisurely look at the bootstrap, the jacknife and cross-validation. *Amer. Statist.,* **37,** 36–48.

Gibson, C. H., C. A. Friehe, and S. O. McConnell, 1977: Structure of sheared turbulent fields. *Phys. Fluids,* **20**(Suppl.), S156–167.

Gregg, M. C., 1987: Structures and fluxes in a deep convecting mixed layer. *Dynamics of the Oceanic Mixed Layer,* P. Muller and D. Henderson, Eds., Hawaii Institute of Geophysics Special Publication 1987, 1–23.

Haugen, D. A., J. C. Kaimal, and E. F. Bradley, 1971: An experimental study of Reynolds stress and heat flux in the atmospheric surface layer. *Quart. J. Roy. Meteor. Soc.,* **97,** 168–180.

Huang, N. D., 1986: An estimate of the influence of breaking waves on the dynamics of the upper ocean. *Wave Dynamics and Radio Probing of the Ocean Surface,* O. M. Phillips and K. Hasselmann, Eds., Plenum Press, 295–313.

Imberger, J., 1985: The diurnal mixed layer. *Limnol. Oceanogr.,* **30,** 737–770.

Khundzhua, G. G., A. M. Gusev, Ye. G. Andreyev, V. V. Gurov, and N. A. Skorokhvatov, 1977: Structure of the cold surface film of the ocean and heat transfer between the ocean and the atmosphere. *Izv. Atmos. and Oceanic Phys.,* (Engl. Transl.), **13,** 506–509.

Kitaigorodskii, S. A., M. A. Donelan, J. L. Lumley, and E. A. Terray, 1983: Wave-turbulence interactions in the upper ocean. Part 2: Statistical characteristics of wave and turbulent components of the random velocity field in the marine surface layer. *J. Phys. Oceanogr.,* **13,** 1988–1999.

Large, W. G., and S. Pond, 1981: Open ocean momentum flux measurements in moderate to strong winds. *J. Phys. Oceanogr.,* **11,** 324–336.

Lombardo, C. P., and M. C. Gregg, 1989: Similarity scaling of viscous and thermal dissipation in a convecting surface boundary layer. *J. Geophys. Res.,* **94,** 6273–6284.

Paulson, C. A., and J. J. Simpson, 1981: The temperature difference across the cool skin of the ocean. *J. Geophys. Res.,* **86,** 11 044–11 054.

Shay, T. J., and M. C. Gregg, 1986: Convectively driven turbulent mixing in the upper ocean. *J. Phys. Oceanogr.,* **16,** 1777–1798.

Soloviev, A. V., 1990: Coherent structures at the ocean surface in convectively unstable conditions. *Nature,* **364,** 157–160.

——, N. V. Vershinsky, and V. A. Bezverchnii, 1988: Small scale turbulence measurements in the thin surface layer. *Deep-Sea Res.,* **35,** 1859–1874.

Stull, R. B., 1988: *An Introduction to Boundary Layer Meteorology.* Kluwer Academic Publishers, 666 pp.

Thorpe, S. A., 1985: Small scale processes in the upper ocean boundary layer. *Nature,* **318,** 519–522.

——, M. Cure, and M. White, 1991: The skewness of temperature derivatives in the oceanic boundary layers. *J. Phys. Oceanogr.,* **21,** 428–433.

Weller, R. A., and J. F. Price, 1988: Langmuir circulation within the oceanic mixed layer. *Deep-Sea Res.,* **35,** 711–747.

Wyngaard, J. C., and O. R. Cote, 1971: The budgets of turbulent kinetic energy and temperature variance in the atmospheric surface layer. *J. Atmos. Sci.,* **28,** 190–201.